

Nematic phase transitions in mixtures of thin and thick colloidal rods

Kirstin Purdy,¹ Szabolcs Varga,² Amparo Galindo,³ George Jackson,³ and Seth Fraden¹

¹*Martin Fisher School of Physics, Brandeis University, Waltham, Massachusetts 02454*

²*Department of Physics, University of Veszprém,*

H-8201 Veszprém, PO Box 158, Hungary

³*Department of Chemical Engineering and Chemical Technology,*

South Kensington Campus, Imperial College London, London SW7 2AZ, UK

(Dated: December 30, 2021)

Abstract

We report experimental measurements of the phase behavior of mixtures of thin (charged semi-flexible fd virus) and thick (fd -PEG created by covalently grafting poly-(ethylene glycol) to the surface of fd virus) rods. The fd -PEG are sterically stabilized but the fd virus are charged, thus varying the ionic strength of a mixture of fd and fd -PEG varies the effective diameter of the bare fd rods, and the effective diameter ratio ($d \equiv D_{fd\text{-PEG}}/D_{fd}$). We examine the phase diagrams of the rod mixtures and find isotropic-nematic, isotropic-nematic-nematic and nematic-nematic coexisting phases with increasing concentration. In stark contrast to predictions from earlier theoretical work, we observe a nematic-nematic coexistence region bound by a lower critical point. Moreover, we show that a rescaled Onsager-type theory for binary hard rod mixtures qualitatively describes the observed phase behavior.

PACS numbers: 64.70.Md, 61.30.St, 61.30.Dk

The entropy driven phase transition of monodisperse suspensions of purely repulsive rods from an isotropic to an aligned nematic phase has been extensively studied experimentally [1, 2], theoretically [3, 4], and computationally [5]. Binary mixtures of hard particles of different aspect ratios and/or shape can exhibit a much richer phase behavior. Quantitatively studying a binary hard-rod mixture is the first step towards understanding the impact of size polydispersity on the phase separation of concentrated suspensions of rodlike macromolecules. Length and diameter polydispersity are prevalent in suspensions of many synthetic and biological rodlike particles including F-actin, microtubules, and DNA. Theoretical studies of binary hard-rod mixtures predict that in addition to isotropic-nematic (I-N) coexistence, isotropic-nematic-nematic (I-N-N), isotropic-isotropic (I-I), and nematic-nematic (N-N) coexistence are possible when the length or diameter ratio of the particles is large enough [6, 7, 8, 9, 10, 11, 12]. However, the topology of the theoretical phase diagram of binary mixtures of rods, including the progression of the phase behavior from a totally miscible nematic to a demixed N-N state and the related existence of N-N critical points, is a subject of considerable debate as the predicted phase behavior of the more concentrated phases (N-N and I-N-N) is extremely sensitive to the approximations employed [8, 9, 12, 13, 14]. The focus of past experimental studies has been on binary mixtures of rods of varying length where I-N, I-N-N and N-N coexistence have been measured [2, 15, 16, 17]. Because of polydispersity in the particle size, high solution viscosity and/or weak attractions these measurements were constrained to low concentrations near the I-N transition [2, 15, 17]. As a consequence, experimental studies of N-N phase behavior are rare. In this Letter, we present experimental measurements of the phase behavior of binary mixtures of rods of varying *diameter* ratio and equal length to very high (nematic) concentrations. These rods are strongly repulsive and highly monodisperse. By examining the phase diagrams well into the nematic region, we find a lower critical point in the N-N coexistence where previously only an upper critical point had been predicted. We compare these unexpected results to the predictions of a scaled Onsager theory [12].

The theory describing the liquid crystal phase behavior of binary rod mixtures is closely related to the theory of orientational ordering developed by Onsager for monodisperse rods [3]. Onsager showed that the decrease in orientational entropy accompanying the formation of an aligned nematic phase is more than compensated for by an increase in the free volume entropy of the rods. The I-N phase transition predicted for monodisperse rods is in excellent

agreement with experiments [1]. By extending Onsager’s theory for the free energy of hard rigid rods in the limit of the second virial coefficient (second virial theory, or SVT) to binary mixtures [3], the phase behavior has been determined for binary mixtures of rods of different diameter [9], and different length [7, 8, 14]. Onsager’s second virial expansion of the free energy is, however, quantitatively accurate only for dilute suspensions of particles of large aspect ratio. For concentrated phase transitions (such as a N-N transition), both “end-effects” due to the finite size of the rods (typically neglected for Onsager-limit studies) and higher virial coefficients are significant, even in the limit of large aspect ratio. Therefore, to study the phase behavior of binary mixtures of rods of short, experimentally accessible, aspect ratios and to describe the phase behavior at high concentrations, we adopt a Parsons-Lee (P-L) free energy [18, 19] as applied to mixtures of rigid rods by Varga *et al.* [12]. The P-L approach approximates higher virial coefficients by interpolating between the Carnahan-Starling free energy for hard spheres and the Onsager free energy for long hard rods. The free energy is described by:

$$\frac{\beta F}{N} = \text{const} + \sum_{i=1}^2 x_i (\ln(x_i \rho) + \sigma(f_i)) + \frac{\beta F_{\text{exc}}^{\text{HS}}}{N 8 v_{\text{HS}}} \sum_{i=1}^2 \sum_{j=1}^2 \langle v_{ij} \rangle$$

Here $\rho = (N_1 + N_2)/V$ is the total number density, x_i and $f_i(\Omega)$ are the mole fraction and orientational distribution function of rods of type i , respectively, and σ is the single particle orientational entropy [12]. In the second term, $F_{\text{exc}}^{\text{HS}}$ is the residual free energy of a system of equivalent hard spheres of volume $v_{\text{HS}} = (x_1 v_1 + x_2 v_2)$ [12], and v_i is the volume of rod i . Furthermore, $\langle v_{ij} \rangle = \int \int x_i x_j v_{ij}(\Omega_1, \Omega_2) f_i(\Omega_1) f_j(\Omega_2) d\Omega_1 d\Omega_2$ is the full orientationally averaged excluded volume (v_{ij}) between rods i and j , with Ω being the orientational unit vector (polar and azimuthal angles). The end-effects are included the excluded volume term [12]. The theoretical phase diagrams presented here are calculated numerically with this free energy functional using techniques previously described [12].

Mixtures of two well characterized systems: the charged semiflexible *fd* virus [1] and *fd* virus irreversibly coated with the neutral polymer poly(ethylene glycol) (PEG) [20, 21] are investigated experimentally. The bare *fd* virus will serve as our thin rod, while the polymer coated *fd* (*fd*-PEG) will be our thick rod. The *fd* virus is grown and purified as previously described [22], and it is characterized by its length $L = 880$ nm, diameter $D = 6.6$ nm, molecular weight $M_w = 1.64 \times 10^7$ g/mol, and persistence length, defined as the length over

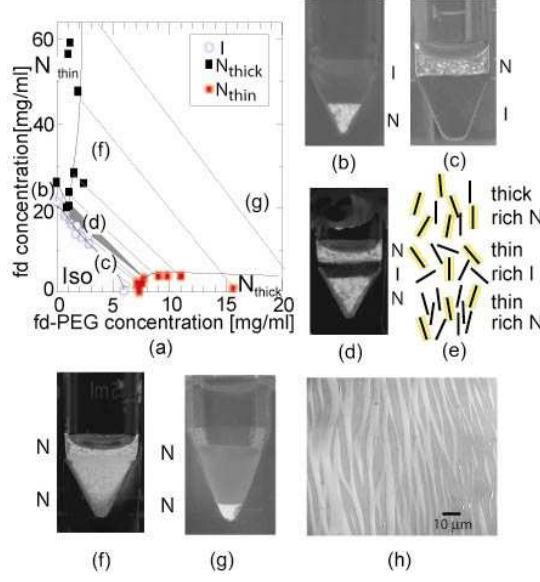


FIG. 1: (Color Online) Phase separation of mixtures of *fd* and *fd*-PEG (20,000 M_w PEG) at 110 mM ionic strength ($d = 3.7$), pH 8.2. The phase diagram is presented in (a). The dark curves are guides to the eye representing the phase boundaries of the two nematic phases and the isotropic phase. The dashed lines indicate coexisting samples, and the three phase region is indicated by the grey triangle. The coexisting phases labeled in (a) as viewed under crossed polarizers are: (b) I-N coexistence; (c) highly fractionated I-N coexistence; (d) I-N-N three phase coexistence with a schematic representation of the partitioning of thick and thin rods shown in (e); (f) N-N demixing just above the triphasic region; and (g) highly concentrated N-N coexistence showing strong partitioning of the thick (yellow, *fd*-PEG) and thin (white, *fd*) rods. The isotropic phase appears dark and the nematic phase appears light due to its birefringence. The yellow color is due to the dye on the *fd*-PEG rods. (h) Differential interference contrast microscopy image of low density *fd*-PEG-rich nematic tactoids in coexistence with high density *fd*-rich nematic bulk phase.

which the tangent vectors along a polymer are correlated, of $P = 2.2 \mu\text{m}$ [1]. The *fd* rods also have a linear surface charge of $10 \text{ e}^-/\text{nm}$ at pH 8.2, thus to compare the phase behavior of *fd* with predictions for hard rods the electrostatic interactions are incorporated into an effective diameter D_{eff} which is larger than the bare diameter and increases with decreasing ionic strength [3, 23]. Over a wide range of ionic strengths, monodisperse suspensions of *fd* are known to undergo an isotropic to cholesteric (chiral nematic) phase transition which is accurately described by SVT for semiflexible hard rods of diameter D_{eff} [1]. Because the free energy difference between the cholesteric and nematic phases is small, comparison with theories developed for nematic phases is appropriate [24].

The thick rods are formed by attaching an amino-reactive PEG, $M_w = 20000 \text{ g/mol}$ (SSA-PEG20K, Shearwater Polymer Corp.), to the exposed amino termini of the viral coat

proteins. The dense polymer coating of approximately 200 ± 30 PEG20K molecules per *fd* [21] acts as a steric stabilizer above an ionic strength of 2 mM. In this regime the isotropic-nematic (cholesteric) phase transition of monodisperse suspensions of *fd*-PEG is independent of ionic strength [20]. The diameter D_{thick} of the thick (virus+polymer) *fd*-PEG rods is thus calculated from the monodisperse isotropic coexistence concentration (c_i) using the theoretical relationship $c_i[\text{mg/ml}] = 222/D_{\text{thick}}[\text{nm}]$, as calculated from SVT adapted for semiflexible rods [20, 25]. D_{thick} varies from 25-40 nm depending on the *fd*/SSA-PEG20K reaction conditions. Rods with different D_{thick} were used separately.

Samples are prepared at multiple virus compositions and concentrations to determine the phase behavior of mixtures of *fd* and *fd*-PEG. The virus suspensions are dialyzed against 20 mM Tris-HCl buffer at pH 8.15 with NaCl added to change the ionic strength such that the diameter ratio $D_{\text{thick}}/D_{\text{thin}} \equiv d$, where $D_{\text{thin}} = D_{\text{eff}}$, varied from $1.1 < d < 3.7$. The observed phase separation includes either an isotropic phase (I) coexisting with a nematic (N) phase, I-N-N three-phase coexistence, or N-N coexistence. The coexisting phases, as viewed under crossed polarizers, are depicted in Fig. 1. This confirms the theoretical predictions for the stable coexisting phases for such a system [9, 12]. Phase separation between two isotropic phases (I-I) is not observed, presumably because d is not large enough. In Figs. (1c) and (1d) the *fd*-PEG-rich nematic phase can be seen to float above the *fd*-rich isotropic phase. Even though the volume fraction of rods is higher in the nematic phase, the mass density of the *fd* rich isotropic phase is greater than that of the *fd*-PEG rich nematic phase. The mass density difference arises in part because of the difference in single particle densities $\rho = 1.35$ g/ml for *fd* and $\rho = 1.007$ g/ml for *fd*-PEG. After equilibration, the concentrations of *fd* and *fd*-PEG in the coexisting phases are measured by absorption spectrophotometry. The optical density (A) of *fd* is $A_{3.84\text{ml/mg}}^{269\text{nm}}$ for samples 1 cm thick. To independently measure the concentrations of thin and thick rods in the coexisting phases, *fd*-PEG is also labeled with the fluorescent dye fluorescein isothiocyanate (FITC) which has an optical density of $A_{68000\text{L/mol}}^{495\text{nm}}$. Before bulk separation of coexisting phases occurs, phase separation on a micron length scale can easily be seen using fluorescence and/or polarization microscopy as shown in Fig. 1h.

In Fig. 2 we present the experimental phase diagrams of the binary mixtures of *fd* and *fd*-PEG at three ionic strengths; corresponding to diameter ratio d ranging from $1.1 < d < 3.0$. For large diameter ratios, $d > 3.0$, marked partitioning is seen in the I-N coexistence region,

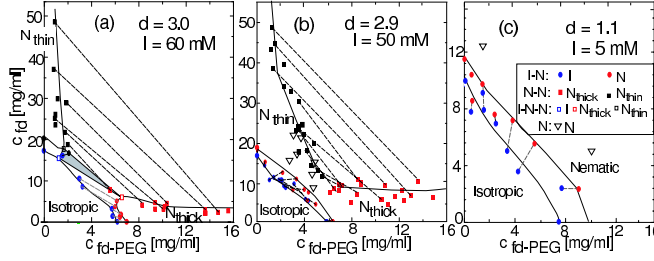


FIG. 2: (Color Online) Phase diagrams of suspensions of *fd*-PEG (20,000 M_w PEG) mixed with *fd* at (a) 60 mM, (b) 50 mM, (c) 5 mM ionic strength, pH 8.2. The legend for all three diagrams is in (c). The dark curves are guides to the eye representing the phase boundaries of the two nematic phases and the isotropic phase. The dashed lines indicate coexisting samples, and open triangles are single phase nematic samples as determined by fluorescence microscopy. The three phase region is indicated by the grey triangle.

as indicated by tie lines in the I-N coexistence region which do not pass through the origin. With increasing overall concentration, a triangular I-N-N three phase region and a N-N coexistence region are found (Fig. 2a). Almost complete partitioning of the thick (*fd*-PEG) and thin (*fd*) rods is observed in the N-N coexistence region. As d decreases, the I-N-N coexistence region becomes smaller, and below about $d = 3.0$ the triphasic region vanishes. Between $d \sim 3.0$ and $d \sim 2.0$ the N-N coexistence is still present at high concentrations, even in the absence of a well defined I-N-N triangle, suggesting a N-N region bounded by a lower critical point. Partitioning of the *fd* and *fd*-PEG between isotropic and nematic phases also decreases in the absence of an I-N-N region, as indicated by the shortening of the I-N tie lines which do not radiate from the origin from Fig. 2b to 2c. For diameter ratios below $d \sim 2.0$ only a single nematic phase is observed.

To shed light on the measured phase separation, we present the predictions for the phase behavior from P-L theory [12] in Fig. 3. Four distinct types of phase diagrams (indicated by the Greek symbols) are predicted for a mixture of rod-like particles of equal length as a function of the diameter ratio and the length of the thick rods. The qualitative evolution of the phase behavior as a function of d for $L/D_{\text{thick}} = 24$, which corresponds to the experimental aspect ratio of the thick rods, is displayed in Fig. 3b-d. The region of I-I coexistence (δ) is not observed experimentally and is not discussed here. For small d , corresponding to region α , a transition from an isotropic to homogenous nematic phase is predicted at low concentrations and a N-N coexistence region bounded by a lower critical point is predicted at high concentrations (Fig. 3b). Region α confirms that an I-N-N coexistence region is not required for the existence of a region of N-N coexistence, as experimentally observed (Fig.

2b). As d increases within region α the N-N lower critical point moves to lower rod concentrations. Region β is characterized by a phase diagram which exhibits an I-N-N coexistence region capped by a region of N-N coexistence bounded by an upper critical point, with an additional region of N-N coexistence bounded by a lower critical point (Fig. 3c). Upon increasing d , these two regions of N-N coexistence coalesce to form a single N-N coexistence region (region γ , Fig. 3d).

The phase diagram for region γ is qualitatively similar to that predicted by SVT [9] for $d > 4.3$, and is experimentally observed for $d \geq 3$ (Fig. 2a). The phase diagrams characterizing regions α and β , however, are qualitatively different from those predicted in the SVT ($L/D \rightarrow \infty$) [9] because they predict a region of N-N coexistence bounded by a lower critical point. Only an N-N coexistence region bounded by an upper critical point is predicted in the SVT for $3.8 < d < 4.3$ [9]. However, it is precisely this N-N coexistence region bounded by a lower critical point which is measured in the $fd+fd$ -PEG solutions (Fig. 2b) for $3 > d > 2$. Simply by extrapolating between the Onsager limit ($L/D \rightarrow \infty$) and the Carnahan-Starling hard sphere limit ($L/D \rightarrow 1$) [18], the P-L scaling [12] qualitatively reproduces the experimental phase diagram for $3 > d > 2$ while SVT alone does not.

Comparing the evolution of experimental phase behavior with d for our long semiflexible rods with the P-L predictions we find that it qualitatively follows the phase behavior predicted for short rigid rods, $L/D_{\text{thick}} \lesssim 7$. In this case, region β is bypassed and the N-N region bounded by the lower critical point coalesces directly with the I-N region creating an I-N-N coexistence region. It has been shown in simulations that the excluded volume of a flexible rod is equivalent to the excluded volume of a shorter but thicker rigid rod [26]. Thus we expect long flexible rods to exhibit a phase behavior similar to that predicted for shorter rigid rods, as observed. Additionally, we observe that the experimental I-N-N coexistence is stable to much lower diameter ratios, $d \sim 3$, than predicted. We suggest that this is because the thin-thick rod interactions are non-additive. Because D_{thin} is defined by electrostatic repulsion, nothing prevents the polymer coated virus (thick rods) from touching the bare surface of the fd (thin rods). Subsequently, the thin-rod interaction diameter is effectively smaller (d is effectively larger). Theoretically, one of the challenges that remains is to incorporate non-additivity and flexibility into theories for the binary rod phase behavior.

In conclusion, we have studied the phase behavior of the first experimental system of thick and thin rods. Onsager's SVT qualitatively reproduces the main features seen in our

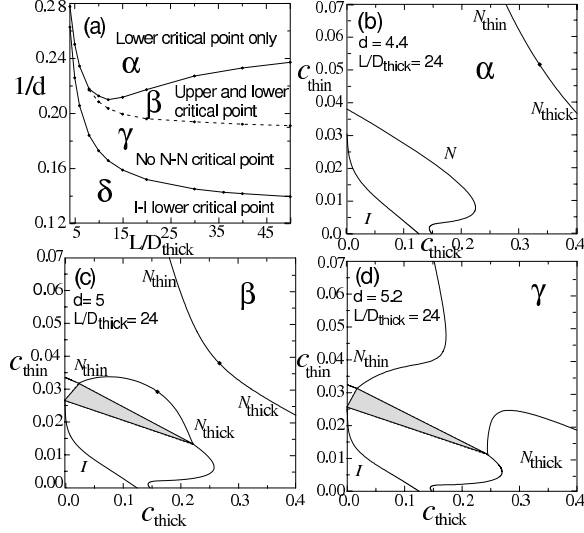


FIG. 3: (a) Characterization of the binary phase behavior of rods of equal length obtained with P-L scaling of the Onsager free energy as a function of the inverse diameter ratio $1/d$ and L/D_{thick} . I-N-N coexistence is found below the uppermost line (regions β and γ). Coalescence of the upper and lower N-N critical points occurs at the dashed line (region γ), and I-I-N coexistence becomes stable below the lower line (region δ). For $L/D_{\text{thick}} < 7$, the lower critical point merges with the I-N coexistence region at the uppermost solid line. The phase diagrams are calculated for $L/D_{\text{thick}} = 24$ with $d = 4.4$ (b), $d = 5$ (c), and $d = 5.2$ (d). Phase diagrams are presented as a function of reduced concentration $c_i = v_i N_i/V$. Three phase coexistence is indicated by the grey triangle.

experimental binary rod mixtures at large diameter ratios, but does not accurately capture the evolution of the phase behavior from a totally miscible nematic to a demixed nematic-nematic state. By incorporating the higher virial coefficients in an approximate fashion with the Parsons-Lee scaling of the free energy for hard rods [12], we proposed an evolution of the binary rod phase diagram with diameter ratio which qualitatively describes the experimental findings. Our experimental and theoretical results show that an I-N-N coexistence region is not required for the existence of a region of N-N coexistence in contrast to past predictions. However, the N-N upper critical point, which is predicted for very long rods in both the SVT and Parsons-Lee theory has not yet been observed experimentally; further experimental or computational studies of binary mixtures of longer, more rigid rods, may reveal this upper critical point.

The experimental research (KP and SF) was supported by an NSF/DMR grant. The theoretical work (AG and GJ) was supported by the Engineering and Physical Sciences Research Council, the Joint Research Equipment Initiative, and the Royal Society-Wolfson

Foundation. We acknowledge Rene van Roij for helpful discussions and unpublished theoretical results.

-
- [1] S. Fraden, in *Observation, Prediction, and Simulation of Phase Transitions in Complex Fluids*, edited by M. Baus, L. F. Rull, and J. P. Ryckaert (Kluwer Academic, Dordrecht, 1995), pp. 113–164.
 - [2] T. Sato and A. Teramoto, *Adv. in Poly. Sci.* **126**, 85 (1996).
 - [3] L. Onsager, *Ann. NY Acad. Sci.* **51**, 627 (1949).
 - [4] G. J. Vroege and H. N. W. Lekkerkerker, *Rep. Prog. Phys.* **55**, 1241 (1992).
 - [5] P. G. Bolhuis and D. Frenkel, *J. Chem. Phys.* **106**, 668 (1997).
 - [6] A. Abe and P. J. Flory, *Macromolecules* **11**, 1122 (1978).
 - [7] H. N. W. Lekkerkerker *et al.*, *J. Chem. Phys.* **80**, 3427 (1984).
 - [8] G. J. Vroege and H. N. W. Lekkerkerker, *J. Phys. Chem.* **97**, 3601 (1993).
 - [9] R. van Roij, B. Mulder, and M. Dijkstra, *Physica A* **261**, 374 (1998).
 - [10] P.C.Hemmer, *Molecular Physics* **96**, 1153 (1999).
 - [11] A. Speranza and P. Sollich, *J. Chem. Phys.* **117**, 5421 (2002).
 - [12] S. Varga, A. Galindo, and G. Jackson, *Molecular Physics* **101**, 817 (2003).
 - [13] R. van Roij and B. Mulder, *J. Chem. Phys.* **105**, 11237 (1996).
 - [14] S. Varga and I. Szalai, *Phys. Chem. Chem. Phys.* **2**, 1955 (2000).
 - [15] T. Itou and A. Teramoto, *Polymer Journal* **16**, 779 (1984).
 - [16] K. Kajiwara *et al.*, *Makromol. Chem.* **187**, 2883 (1986).
 - [17] H. N. W. Lekkerkerker *et al.*, in *Observation, Prediction and Simulation of Phase Transitions in Complex Fluids*, edited by M. Baus, L. F. Rull, and J. P. Ryckaert (Kluwer Academic, Dordrecht, 1995), pp. 53–112.
 - [18] J. D. Parsons, *Phys. Rev. A* **19**, 1225 (1979).
 - [19] S. Lee, *J. Chem. Phys.* **87**, 4972 (1987).
 - [20] Z. Dogic and S. Fraden, *Phil. Trans. R. Soc. Lond. A.* **359**, 997 (2001).
 - [21] E. Grelet and S. Fraden, *Phys. Rev. Lett.* **90**, 198302 (2003).
 - [22] J. Sambrook and D. W. Russell, *Molecular Cloning: A Laboratory Manual* (Cold Spring Harbor Laboratory, New York, 2001), 3rd ed.

- [23] A. Stroobants, H. N. W. Lekkerkerker, and T. Odijk, *Macromolecules* **19**, 2232 (1986).
- [24] P. G. de Gennes and J. Prost, *The Physics of Liquid Crystals* (Oxford Science, 1993), 2nd ed.
- [25] Z. Y. Chen, *Macromolecules* **26**, 3419 (1993).
- [26] H. Fynewever and A. Yethiraj, *J. Chem. Phys.* **108**, 1636 (1998).